LUND UNIVERSITY

Spectroscopic studies of wood-drying processes

Andersson, Mats; Persson, Linda; Sjöholm, Mikael; Svanberg, Sune

Published in:
Optics Express

2006

Link to publication

Citation for published version (APA):
Andersson, M., Persson, L., Sjöholm, M., & Svanberg, S. (2006). Spectroscopic studies of wood-drying processes. *Optics Express*, *14*(8), 3641-3653. http://www.opticsinfobase.org/abstract.cfm?URI=oe-14-8-3641

Total number of authors:
4

General rights
Unless other specific re-use rights are stated the following general rights apply:
Copyright and moral rights for the publications made accessible in the public portal are retained by the authors and/or other copyright owners and it is a condition of accessing publications that users recognise and abide by the legal requirements associated with these rights.
• Users may download and print one copy of any publication from the public portal for the purpose of private study or research.
• You may not further distribute the material or use it for any profit-making activity or commercial gain
• You may freely distribute the URL identifying the publication in the public portal

Read more about Creative commons licenses: https://creativecommons.org/licenses/

Take down policy
If you believe that this document breaches copyright please contact us providing details, and we will remove access to the work immediately and investigate your claim.

LUND UNIVERSITY

PO Box 117
221 00 Lund
+46 46-222 00 00

Spectroscopic studies of wood-drying processes

Mats Andersson, Linda Persson, Mikael Sjöholm, and Sune Svanberg

Atomic Physics Division, Lund Institute of Technology,
P.O. Box 118, S-221 00 Lund, Sweden
sune.svanberg@fysik.lth.se

Abstract: By the use of wavelength-modulation diode laser spectroscopy, water vapor and oxygen are detected in scattering media nonintrusively, at 980 nm and 760 nm, respectively. The technique demonstrated is based on the fact that free gases have extremely sharp absorption structures in comparison with the broad features of bulk material. Water vapor and oxygen measurements have been performed during the drying process of wood. The results suggest that the demonstrated technique can give information about the drying process of wood to complement that of commercially available moisture meters. In particular, the time when all the free water has evaporated from the wood can be readily identified by a strong falloff in the water vapor signal accompanied by the reaching of a high-level plateau in the molecular oxygen signal. Furthermore, the same point is identified in the differential optical absorption signal for liquid water, with a sharp increase by an order of magnitude in the ratio of the signal intensities at 980 nm and 760 nm.

© 2006 Optical Society of America

OCIS codes: (000.2190) Experimental physics; (300.6260) Diode laser spectroscopy; (290.7050) Turbid media

References and links

1. J. M. Dinwoodie, "*Timber: Its nature and behaviour*," (E & FN, 2000).
2. B. Berglund, B. Brunekreef, H. Knöppel, T. Lindvall, M. Maroni, L. Mølhave, and P. Skov, "Effects of indoor air pollution on human health," Indoor Air **2**, 2–25 (1992).
3. S. Joseph Cohen and T C.S Yang, "Progress in food dehydration," Trends in Food Science & Technology **6**, (1995).
4. D. A. Skoog and M.D. West, "*Fundamentals of Analytical Chemistry*," 7th edition, (Saunders, 1995).
5. G.Müller, B. Chance, R. Alfano, S. Arridge, J. Beuthan, E. Gratton, M. Kaschke, B. Masters, S. Svanberg, and P. van der Zee, eds., "Medical optical tomography, functional imaging and monitoring," in *SPIE Institute Series*, Vol. **11**, (SPIE, 1993).
6. C. Abrahamsson, J. Johansson, S. Andersson-Engels, S. Svanberg, and S. Folestad, "Time-resolved NIR spectroscopy for quantitative analysis of intact pharmaceutical tablets," Anal. Chem. **77**, 1055–1059 (2005).
7. T. J. Farrell, M. S. Pattersson, and B. Wilson, "A diffusion theory model of spatially resolved, steady-state diffuse reflectance for noninvasive determination of tissue optical properties in vivo," Med. Phys. **19**, 879–888 (1992).
8. M. S. Pattersson, B. Chance, and B. C. Wilson, "Time-resolved reflectance and transmittance for the noninvasive measurement of tissue optical properties," Appl. Opt. **28**, 2331–2336 (1989).
9. C. af Klinteberg, A. Pifferi, S. Andersson-Engels, R. Cubeddu, and S. Svanberg, "In vivo absorption spectroscopy of tumor sensitizers using femtosecond white light," Appl. Opt. **44**, 2213–2220 (2005).
10. M. Sjöholm, G. Somesfalean, J. Alnis, S. Andersson-Engels, and S. Svanberg, "Analysis of gas dispersed in scattering media," Opt. Lett. **26,** 16–18 (2001).
11. J. Alnis, B. Anderson, M. Sjöholm, G. Somesfalean, and S. Svanberg, "Laser spectroscopy on free molecular oxygen dispersed in wood materials," Appl. Phys. B **77**, 691–695 (2003).

#67781 - $15.00 USD Received 3 February 2006; revised 28 March 2006; accepted 3 April 2006
(C) 2006 OSA

12. L. Persson, H. Gao, M. Sjöholm, and S. Svanberg, "Diode laser absorption spectroscopy for studies of gas exchange in fruits," Opt. Lasers Eng. **44**, 687–698 (2006).
13. L. Persson, B. Anderson, M. Andersson, M. Sjöholm, and S. Svanberg, "Studies of gas exchange in fruits using laser spectroscopic techniques," in Proceedings of Fruitic05 Symposium (Montpellier, France, September 12-16, 2005).
14. G. Somesfalean, M. Sjöholm, J. Alnis, C. af Klinteberg, S. Andersson-Engels, and S. Svanberg, "Concentration measurement of gas imbedded in scattering media employing time and spatially resolved techniques," Appl. Opt. **41**, 3538–3544 (2002).
15. L. Persson, K. Svanberg, and S. Svanberg, "On the potential of human sinus cavity diagnostics using diode laser gas spectroscopy," Appl. Phys. B **82,** 313–317 (2006).
16. L. Sandra, B. Roderick, and M. L. Roderick, "Plant-water relations and the fibre saturation point," New Phytol. **168**, 25–37 (2005).
17. P. Perré, "The role of wood anatomy in the drying of wood: Great Oaks from little acorns grow," 8th Int. IUFRO Wood Drying Conference (Brasov, Rumania, August 24–29, 2003).
18. M. Goyeneche, D. Lasseux, and D. Bruneau, "A film-flow model to describe free water transport during drying of a hydroscopic capillary porous medium," Transp. Porous Media **48**, 125-158 (2002).
19. L. James, "Electric moisture meters for wood," Gen. Tech. Rep. FPL-GTR-6. Madison, WI: U.S. Department of Agriculture, Forest Service, Forest Products Laboratory, 1988.
20. H. Forsén and V. Tarvainen, "Accuracy and functionality of hand held wood moisture content meters," VTT Publications 420 (2000).
21. P. J. Wilson, "Accuracy of a capacitance-type and three resistance-type pin meters for measuring wood moisture content," Forest Products Journal, **49**, 29–32 (1999).
22. C. Nordling and J. Österman, "*Physics Handbook*," 4th ed. (Studentlitteratur, 1987).
23. S. Matcher, M Cope, and D. Delpy, "Use of the water absorption spectrum to quantify tissue chromophore concentration changes in near infrared spectroscopy," Phys. Med. Biol. **39,** 177–196 (1994).
24. T. Svensson, J. Swartling, P. Taroni, A. Torricelli, P. Lindblom, C. Ingvar, and S. Andersson-Engels, "Characterization of normal breast tissue heterogeneity using time-resolved near-infrared spectroscopy," Phys. Med. Biol. **50,** 2559–2571 (2005).

1. Introduction

Drying processes, i.e., the removal of moisture from materials, are of utmost importance in many industrial contexts and everyday experiences. For instance, wood needs to be dried from its natural moisture before its use as a fuel or as a construction material [1]. An important issue is that moisture in building materials induces mold, especially if the ventilation is insufficient, which is of major concern in the building sector [2]. Grain and cereals need drying for storage and for further processing in the food industry [3]. Paper processing includes important drying steps as is the case also in many further industrial processes.

Many natural materials are porous and hydrophilic. The pores can be filled with air or other gases, but may also be partially or fully filled with water; a frequently undesired situation. Capillary action is an important passive process when porous materials take up water. Materials frequently swell (increase in volume) when wet. In nonporous media the process of osmosis is in action. If the material has some rigid scaffolding structure, such as wood and other building materials, the swelling is minor. Then the pores originally filled with air instead become water filled. By increasing the vapor pressure of water by heating in combination with securing an environment with reduced relative humidity, forced drying can be achieved.

The status of drying materials is often studied by handheld moisture meters that measure the water content by an indirect method relying on the fact that the electrical properties of the material is dependent on the water content. However, these instruments are not able to monitor the whole drying process and are in some cases intrusive. Recent developments in diode-laser-based spectroscopy pose an interesting alternative approach, which would be to monitor the water vapor as well as the liquid water by a more direct, noninstrusive spectroscopic approach.

The present paper deals with the study of drying of wood using high-resolution near-IR laser absorption spectroscopy. A tunable diode laser operating close to 980 nm is used to monitor gaseous water. Liquid water also exhibits a broad absorption peak in the same wavelength

#67781 - $15.00 USD Received 3 February 2006; revised 28 March 2006; accepted 3 April 2006
(C) 2006 OSA

region. For reference, atmospheric oxygen gas in the pores is also monitored in its A band close to 760 nm. This wavelength also provides a convenient off-resonance wavelength in the liquid-water spectrum for assessment of liquid-water contents.

Absorption spectroscopy is a very common method for measuring concentrations of substances utilizing the Beer–Lambert law and a suitable calibration procedure (See, e.g., [4]). However, the application of this method is not straightforward for natural materials such as wood, since the fact that they are inhomogeneous and porous also means that they are highly scattering, making the optical pathlength through the sample undefined. This situation is common in medical optics, where scattering and absorption are intertwined [5], as is also the case in analytical spectroscopy of pharmaceutical preparations [6]. Different techniques for handling multiple scattering of light have been developed for assessing the concentration of liquid and solid absorbing constituents. Spatially separated measurements [7] and time-resolved techniques [8] constitute two main approaches for enabling concentration determinations. A recent example on the determination of tumor sensitizer concentration in vivo is given in Ref. [9].

Such techniques have been extended to free gases present in porous media through the introduction of the Gas in Scattering Media Absorption Spectroscopy (GASMAS) technique [10]. Normally a modest resolution is used in solid-state spectroscopy because of the broad absorbing structures. However, if single-mode diode laser spectroscopy using sensitive modulation techniques is employed, then structures appear that are typically 10,000 times narrower due to free gas. So far, the GASMAS technique was applied to the monitoring of free molecular oxygen in materials as diverse as wood, polystyrene foam, and fruits [10-13]. In particular, gas transport through the media could be studied by first subjecting the material to a pure nitrogen atmosphere and then observing the time constant for the reinvasion of normal ambient (oxygen-containing) air. Concentrations could be determined by combining GASMAS measurements with time-resolved measurement, revealing the time history of the photons inside the sample [14]. The GASMAS technique was also very recently applied to the monitoring of human sinus cavities [15].

The present paper focuses on spectroscopic monitoring of the drying of wood, and the GASMAS technique has in this context been extended to water-vapor monitoring. The structure of wood and the basics of wood-drying processes are presented in the next section. Conventional methods for measuring moisture in wood are discussed in Section 3. The experimental arrangements used in the present work are then presented in Section 4. Measurements and results are described in Section 5. A discussion of the results and conclusions from the study are presented in the final section.

2. Wood structure and its drying process

2.1. Wood structure

Wood has a complicated architecture, described in detailed, e.g., in Ref. [1]. In a tree the wood structure supports the treetop, stores nutritious substances, and transfers minerals and water, which have been absorbed by the root system. Thus, it needs to be strong, hydrophilic, and flexible since a tree grows and lives in a changing environment. Even though there exist hundreds of different types of wood material, they can be divided into two groups, hardwood (deciduous) and softwood (coniferous); see Fig. 1. Hardwood is the most complicated of the two and comprise wood such as balsa, white oak, ash, mahogany, etc. The density of hardwood may vary from about 0.1 to 1.2 g/cm^3, depending on type of wood. Hardwood is characterized by a combination of complicated cell types orientated both vertically, tangentially, and radially. Softwood, on the other hand, is distinguished by a much simpler combination of cells that runs mostly vertically in a tree. Typical examples of wood that belong to the softwood group are spruce, pine, and larch. The weight of softwood may vary from 0.3 to 0.7 g/cm^3.

#67781 - $15.00 USD Received 3 February 2006; revised 28 March 2006; accepted 3 April 2006
(C) 2006 OSA

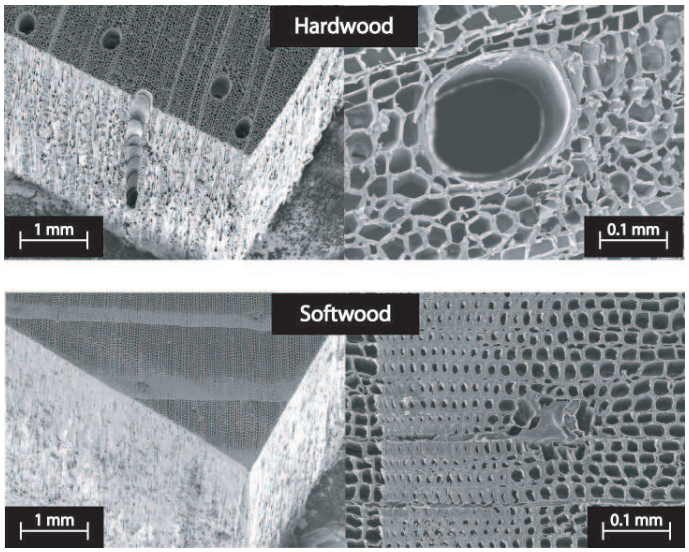

Fig. 1. Microscopic pictures of hardwood (balsa) and softwood (pine).

From a microscopic point of view wood consists of cellular structures that handle tasks carried out in a tree. Water and minerals are stored and transported vertically via cells, forming vessels, and horizontally via cell structures called rays. In total, wood cells can be classified into four different types; parenchyma (storage of nutritients), tracheids (support and conduction), fibers (support), and vessel cells (conduction).

In hardwood all four cell types are present, but tracheids are uncommon. Instead fibers and vessels are responsible for support and conduction of water and minerals. Fibers are usually 1-2 mm long and 10-20 μm wide, and their only function is support. However, vessel cells are about the same length as the fibers but up to 0.5 mm wide. Since the ends of the vessels are situated on top of each other they can make up a long tube. Thus, vessels act as an efficient water tube since the ends of the vessels are more or less dissolved.

In softwood only two cell types are present, namely parenchyma and tracheids. Tracheids are the most common cell type (about 90% of the softwood), and its main function is support and conduction of minerals and water. The size of the cell is about 2–4 mm long and about 30–50 μm wide. It is situated vertically in the tree and conducts water and minerals via small pits located on the cell surface. Parenchyma cells are small, 200 x 30 μm^2 in size, taking care of the storage of nutritients.

2.2. Wood drying processes

All types of wood consist of cellulose, hemicellulose, lignin, and extractives. The density of wood elements is about 1.5 g/cm^3, but since wood is based on a cell structure, with size that differs per type of wood, the density of wood may vary from 0.1 to 1.2 g/cm^3 if the content of water is kept low. However, since the wood cell structure is hydrophilic and full of air, wood is heavily affected by water and moisture.

The moisture content in wood is defined as the ratio between the weight of water in a piece of wood and the weight of the wood when no water is present. This means that the moisture content is higher than 100% in a living tree. During this state water is stored in cells and vessels (free water) but also in cell walls (bound water) that have expanded due to absorbed water.

If a tree is cut into pieces, the moisture content starts to decrease immediately; see Fig. 2.

#67781 - $15.00 USD Received 3 February 2006; revised 28 March 2006; accepted 3 April 2006
(C) 2006 OSA

At first free water is moved to the wood surface by capillary forces where it is evaporated into the atmosphere. Due to the evaporation process the surface temperature is decreased, and heat must be transferred from the environment in order to maintain the drying of the wood.

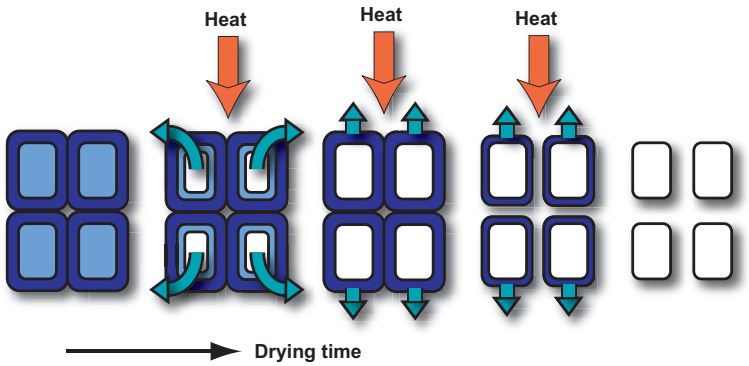

Fig. 2. Wood-drying process. At first the cells are filled with water, but in the end no free water exists, and the absorbed water in cell walls is dried out until an equilibrium state with the surrounding environment is reached.

When all free water has been evaporated the bound water starts to evaporate as well. This state of the wood is known as the fiber saturation point (FSP) and it corresponds to a moisture content of about 25–30%, depending of type of wood. Since bound water is situated inside the cell walls, more energy is needed to evaporate it. Thus, the drying rate decreases and the wood shrinks. In the end of the drying process, the wood reaches an equilibrium state with its environment. The moisture content inside wood depends on temperature and humidity level of the environment. A typical value of the moisture content for dried wood is 12–15% [16-18].

3. Commercially available moisture meters

Handheld electric moisture meters are commonly used to measure the moisture content in wood. The measurement technique was developed in the late 1930's, and today there exists a number of manufacturers that develop and sell handheld moisture meters for measuring, e.g., moisture in wood and concrete. Mainly, two different measurement principles exist: resistance and dielectric type moisture meters [19-21].

The resistance type of moisture meter measures the electric resistance in wood between two pins that are connected at the wood surface or inserted into the wood, with typical distances of centimeters between the pins. If the wood is dry it acts as an isolator, and the resistance is in the order of 10^5 MΩ. However, since water in wood contains ions, the resistance in wood decreases down to about 0.5 MΩ when the moisture content is close to the saturation point.

In order to measure the moisture content using the resistance principal, one has to know the type of wood and from what region it comes. It turns out that all species of wood have different resistance curves even for one type of wood that has grown at two different locations. Today, resistance curves for many species of wood are stored in the device and controlled by a microprocessor.

Although the resistance type of moisture meter is easy to produce and operate, precautions should be considered. At first this measurement method is intrusive. Secondly, the resistance curve for wood is affected by temperature. Thus, a temperature sensor is included in some of the meters. Other disadvantages are the limited measurement range and that the result depends on whether the pins are inserted in parallel or perpendicular to the wood fibers. The upper

#67781 - $15.00 USD Received 3 February 2006; revised 28 March 2006; accepted 3 April 2006
(C) 2006 OSA

limit is set by the fact that above the fiber saturation point (about 25–30% moisture content), the resistance measurement data are not reliable. The lower limit (about 7% moisture content) depends on the difficulties to measure resistance in the order of 10^5 MΩ and above.

The dielectric type of moisture meter uses a nonintrusive measurement technique that measures the dielectric constant of the combined wood and water material. Since the dielectric constant for water is much higher than that of wood (by a factor of 25), the moisture content may be estimated. Anyway, each type of wood has its specific dielectric constant. Specific wood calibration data are stored in the device and controlled by a microprocessor. The dielectric moisture meter is known to have poor performance compared to the resistance type. However, it is commonly used for relative measurements. The surface electrodes are sensitive to other materials close to the surface and density fluctuations of the wood. The measurement range varies from 5% to about 25% moisture content.

4. Setup for diode laser spectroscopy on wood

We will now describe our spectroscopic setup for moisture studies. While measurements using a light transmission or backscattered geometry can be made with the GASMAS method, the former one was chosen because of its simplicity in terms of the optical arrangement and also regarding the signal interpretation. However, a backscattering geometry is attractive in terms of optical access and is also the only possible one for thick samples. Our setup is based on two almost identical arrangements that are run simultaneously. One setup is used for oxygen measurement while the second is used to measure water vapor (moisture) contents in the same piece of wood. A schematic drawing is shown in Fig. 3. The oxygen measurement setup is explained in more detail in Refs. [12]. However, in the present setup the photo multiplier tube (PMT) sensor is replaced by a silicon detector (Photovoltaic PIN-10DP from UDT) with an active surface of 100 mm^2.

The major difference between the oxygen and the water-vapor setup is the wavelength of the diode lasers used. For the oxygen detection a diode laser (Sharp LT031MDO) with a maximum output power of 7 mW, operating at 2 mW at the sample, is used to scan across the R7R7 oxygen line at 761.003 nm (vacuum wavelength). The scan range was typically 20 GHz (0.04 nm). A near-IR Fabry–Pérot diode laser (Specdilas F760) with a maximum output of 200 mW at 980 nm, and efficiently operating at 40 mW at the sample, is used as a spectroscopic light source to detect the water-vapor line (vibration; (000)→ (121), rotation; J"=5→ J'=4, K_a"=0→ K_a'=0, K_c"=5→ K_c'=4) at 978.509 nm (vacuum wavelength). The scan range was typically 35 GHz (0.11 nm).

The basis for the measurement is that the wavelength of the laser light is scanned across the absorption lines by sweeping the operating current of the lasers by the use of a 4 Hz saw tooth ramp. To achieve wavelength modulation spectroscopy (WMS) with lock-in detection, the operating current is also modulated by a sinusoidal wave at 9 kHz with a modulation index of about 1 in both cases. The laser light is focused into a fiber that guides the light to the sample. The water vapor setup uses the same type of silicon detector as the one used for oxygen. The output from each detector is split into two signal branches. One, directly connected to an oscilloscope, is referred to as the direct signal, while the second part goes via the lock-in amplifier before being connected to another channel of the oscilloscope, and is referred to as the WMS signal. The data are stored and analyzed using a computer. Typical readings for oxygen and water vapor are shown in the lower part of Fig. 3. The peak-to-peak value of the WMS signal is measured and normalized by dividing with the direct signal value at the corresponding wavelength in order to determine the fractional absorption during the drying process.

As discussed for instance in [10], a method called standard addition, well known in analytical chemistry, is used in order to calibrate a measured normalized WMS signal and transfer it to a

#67781 - $15.00 USD Received 3 February 2006; revised 28 March 2006; accepted 3 April 2006
(C) 2006 OSA

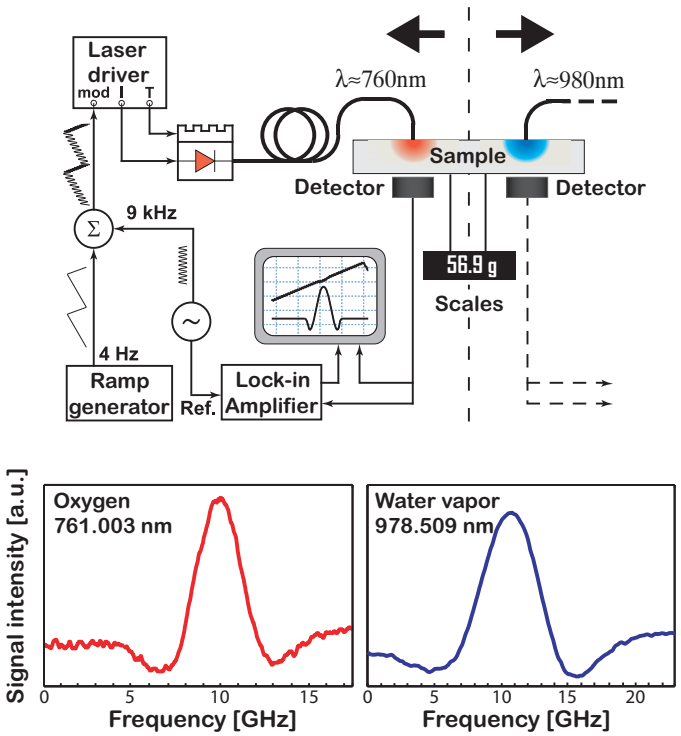

Fig. 3. Schematic drawing of the spectroscopic setup of similar diode laser spectrometers for oxygen (left) and water vapor (right). Typical readings of the WMS signals for oxygen and water vapor in wood are shown in the lower part. The half widths of the signals are of the order of a few GHz in both cases. The half widths at half maximum (HWHM) of the absorption lines are, according to HITRAN, 1.61 GHz for oxygen and 2.72 GHz for water vapor at standard conditions.

more meaningful quantity—a so-called equivalent mean path, L_{eq}. It is determined by adding free air path lengths in the collimated laser beam before it enters the test sample. The equivalent mean path length corresponds to the distance that the light has to travel in ambient air in order to obtain the same signal as in the sample $L_{eq} \cdot c_{air} = \langle L_{sample} \rangle \cdot c_{sample}$, where c_{air} corresponds to the gas concentration in air, $\langle L_{sample} \rangle$ to the mean path length in the sample, and c_{sample} to the gas concentration in the sample. The calibration procedure is carried out by removing the wood sample and placing an optical attenuation filter on top of the detector. A collimator lens was placed at the end of the fiber. The normalized WMS signal was measured for different added air distances between the collimator lens and the filter. A linear function between the normalized WMS signal and added air distance is obtained. This function can then be used to estimate the L_{eq}. The calibrations are done once for each laser, and these calibration curves are used for all experiments. Precautions were taken when the water-vapor WMS signal was calibrated. The room temperature and relative humidity were measured by a hygrometer (Testo 608-H1) sensor and the partial pressure of the water vapor was estimated.

An analog lab scale (Libror EB-280, Shimadzu) is used to measure the weight of the wood in order to calculate the average moisture content during the drying process. At the end of the drying process a commercial convection oven was used to dry the wood at 110^{o}C in order to determine the truly dry weight.

#67781 - $15.00 USD Received 3 February 2006; revised 28 March 2006; accepted 3 April 2006
(C) 2006 OSA

5. Measurements and results

Uniform balsa wood pieces of 10 cm width, 30 cm length, and 0.8 cm thickness derived from the same batch were used in the measurements. The figures of balsa wood shown in Fig. 1 are from the wood samples studied. The wood was kept under water for typically three days and was studied directly after being exposed to the ambient laboratory air. The drying could be followed by reading off the analog scales, onto which the piece of wood was attached.

The results of conventional measurements of the moisture contents during the drying process are shown in Fig. 4, with the instrument applied in a straightforward manner. The weight reading from the scale, expressed as moisture content, is plotted together with data from the resistance and the dielectric moisture meters. It can clearly be seen that the results from the meters poorly describe the real drying process monitored by the scale for moisture content above the FSP. Obviously there is a need for improved measurement techniques for moisture.

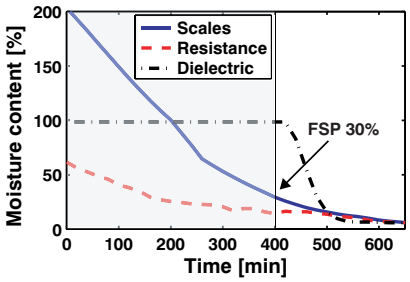

Fig. 4. Measured moisture contents during the drying process of the sample. Curves indicate moisture content (blue curve) when measured by logging the weight of the sample, (red dashed curve) when measured by using a resistance moisture meter (Protimeter Timbermaster), and (black dash-dotted curve) when measured with a dielelectric moisture meter (MC-300W, Exotek). The fiber saturation point (FSP) is indicated in the figure (moisture content=30%).

The temperature of the wood surface was also monitored with thermocouples. The measurements were performed on a different sample. In this case the sample had been soaked in water for a longer time than the case when recording the data in Fig. 4. Typical results are shown in Fig. 5(a), where the blue curve shows a weight loss to a stable value of about 33% of the original wet weight, the dry material plateau being reached after about 1200 min. The drying process is, as expected, accompanied by a lowering of the temperature. During the first 600 min the temperature was stable at 9^{o}C below the ambient value (25^{o}C), which was gradually reached after 1200 min. Local possible heating, due to laser beams, was found to be very small. This results in a marginal increase of water vapor pressure.

Since gaseous water (water vapor) is measured in our study it is interesting to consider the vapor pressure of water as a function of the temperature. The corresponding curve is given in Fig. 5(b). It shows the partial pressure of the vapor in a closed volume containing liquid water at the given temperature. We note that the vapor pressure is increasing by a factor 1.8 when the temperature rises from 16^{o}C to 25^{o}C. We also note that water vapor at ambient temperature only accounts for a small percentage of the mass in normal air. Frequently ambient air does not feature the full water vapor pressure corresponding to the ambient temperature. If there is no air movement and large amounts of distributed liquid water the relative humidity would be 100%, like in a sealed-off volume. Due to the exchange of dryer air, the effective humidity becomes less. Readings of 20–40% relative humidity (percentage of the fully saturated value at the given temperature) are common in indoor environments at wintertime in Sweden.

#67781 - $15.00 USD Received 3 February 2006; revised 28 March 2006; accepted 3 April 2006
(C) 2006 OSA

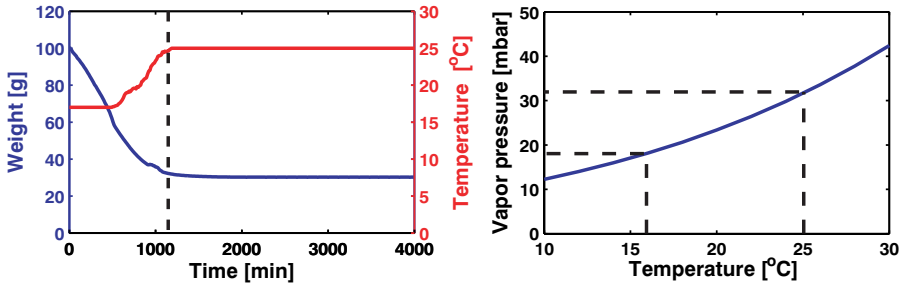

Fig. 5. (a) Measured temperature at the surface of the sample and measured weight during the drying process. (b) Vapor pressure as a function of the temperature [22].

We will now present data from our near-IR laser spectroscopic measurements. We performed simultaneous (molecular) water vapor and molecular oxygen measurements at points separated by about 10 cm on the piece of wood, assuming the material to be laterally uniform. These data were recorded simultaneously as the temperature and weight data in Fig. 5(a). A small air space was left between the sample and the detectors to allow water to homogeneously diffuse out of the sample. The setup is shown in Fig. 3. Oxygen does not have a liquid phase in the temperature range studied (it liquifies at 90K). In contrast, water has a liquid phase as well as a gaseous phase, and the vapor pressure is, as just discussed, temperature dependent.

In understanding the dynamics of wood drying it is useful to first consider the behavior of the molecular oxygen L_{eq} during the drying, which as mentioned before is proportional to the normalized WMS signal. In Fig. 6(a) the fractional oxygen absorption is plotted in red. The signal is proportional to the oxygen concentration times the effective distance travelled through the gas-filled pores, the latter factor being strongly sensitive to the degree of light scattering in the material. The signal is plotted as an equivalent path length in normal air containing 21% oxygen, as previously discussed. It should be noted that the effective path length through the material, useful in a standard Beer–Lambert law view, can be expected to change during the drying process. One aspect is that while liquid water is an index-matching fluid reducing the scattering when the pores are water filled, the scattering should increase when the air-filled inhomogeneities develop during the drying process. We notice that the oxygen signal increases from a non-zero value (there are air-filled pores even in the very wet wood) by a factor of about 8 to then stay constant at the high value, reached at about 1300 min when all the liquid water is driven out and all the pores are instead gas filled.

The simultaneously measured gaseous water signal is included in blue in Fig. 6(a). Again, the curve starts at a non-zero level (corresponding to the presence of gas-filled pores with saturated water vapor also in the very wet wood). The signal increases to a maximum at about 1200 min, reached slightly before the oxygen signal maximum. At the same time as the oxygen signal stays constant the water vapor signal gradually falls off to a steady value of about 25% of the maximum value. This could be interpreted in the following way: Around 1200 min the pores are almost void of water, as indicated by the dashed line in Fig. 5(a), but there is still a sufficient amount of water to sustain the full saturated water vapor partial pressure. Shortly thereafter, this is no longer the case, and the pores with constant volumes and situated in a material with constant scattering properties gradually lose the saturated vapor pressure and gradually attain the relative humidity value of the laboratory, which for the measurement case with an ambient temperature of 25°C was separately measured to 24% with a hygrometer. This is in good agreement with the measured signal falloff to about 25% of the value with

#67781 - $15.00 USD Received 3 February 2006; revised 28 March 2006; accepted 3 April 2006
(C) 2006 OSA

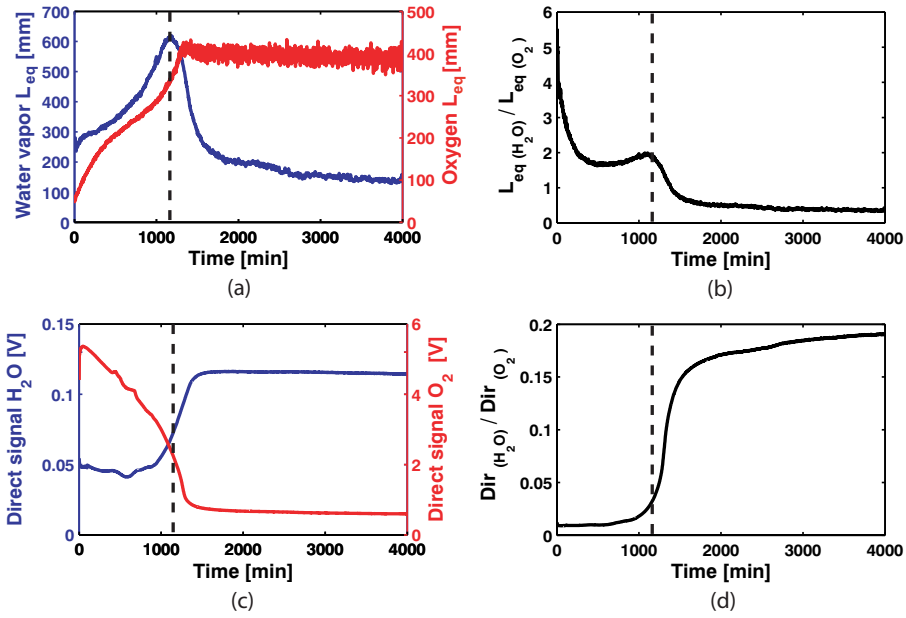

Fig. 6. (a) Equivalent mean path length for water vapor and oxygen during the drying process of balsa. (b) Ratio between detected equivalent mean path length for water vapor and oxygen. (c) Direct signals for water vapor and oxygen during the drying process of balsa. (d) Ratio between detected direct signal for water vapor and oxygen.

full saturation. The displacement of about 100 min between the reaching of the maximum for oxygen and water vapor is compatible with the typical times for air diffusion in balsa wood measured separately [11].

While the above observations are readily interpreted, the detailed behavior of the water vapor signal during the drying is due to many different influences. Let us first state that if two permanent gases such as nitrogen and oxygen had been studied, the same type of behavior (apart from small effects of different diffusivity), i.e., a constant ratio between the signals during the drying phase, would have been expected. This statement has as a prerequisite that the two gases absorb at close-lying wavelengths so that the scattering properties are similar. In contrast to this, the ratio between the water vapor signal and the oxygen signal is strongly varying during the drying process, as can be seen in Fig. 6(b). The temperature increase in the time span 400–1200 min (see Fig. 5, red curve) leads to an acceleration in the water-vapor signal level beyond that for oxygen, for which the concentration is marginally reduced (a few percent) by the temperature increase. This may explain the tendency of increase of the ratio curve toward the end of the drying period. The high initial value in the ratio curve may be related to the time constant for oxygen diffusion through the material also discussed with regard to the different times for the two gases to reach the maximum WMS signal. It should be noted that in the drying up of a pore, the walls of the cavity will be uniformly covered by liquid water due to the surface tension. This may impair the transport of oxygen through the film while the water vapor can freely build up in the central microbubble of the pore, see Fig. 2. Effects of this kind may also influence the balance between the two gases in the cavities during the drying process. As noted, when everything is dry, conditions are static with regard to scattering and the behavior of both curves is clearly understood as discussed above.

So far we have been discussing the fractional absorptive imprint of the gas (intensity on

#67781 - $15.00 USD Received 3 February 2006; revised 28 March 2006; accepted 3 April 2006
(C) 2006 OSA

the absorption line compared to the intensity off the line), which is decisive for concentration measurements based on the Beer–Lambert law. However, it is also interesting to study the dynamics of the total light (off the narrow absorptive features) at the two wavelengths used (980 nm and 760 nm, respectively). Such measurements were performed and the results are shown in Figs. 6(c)–(d) and in Fig. 7. The curves in Fig. 6(c) show a very different behavior with the water signal increasing in the final phase of drying from an almost constant initial level to a final value about 2.5 times higher. On the contrary, the 760 nm signal starts at a high level and, with acceleration, reaches a steady value about 5 times lower when the wood is dry. The ratio of detected direct signal for water and oxygen is shown in Fig. 6(d). In explaining these phenomena it is important to note that liquid water has quite a strong broadband absorption around 980 nm, as detailed in Fig. 7(a) and already noted in the Introduction. We note that this absorption influences the on- and off-resonance frequencies for the narrowband water-vapor signals alike, and does not influence the fractional absorption determining the water-vapor concentration. However, the laser beam is clearly attenuated by the water contents. The initial flat response of the 980 nm curve for the drying wood can be interpreted to mean that the reduction of water during the initial drying is compensated by the increased light path length due to the developing gas-filled pores. Finally, the absorbing liquid water disappears and the detected light settles on a level determined by the attenuation of the light-scattering dry wood.

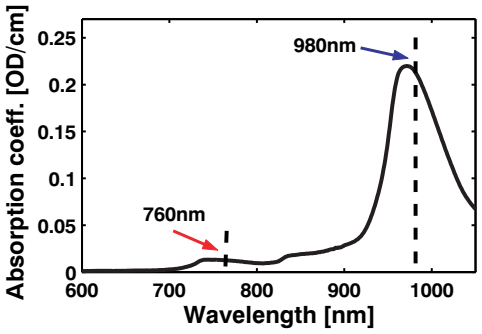

(a)

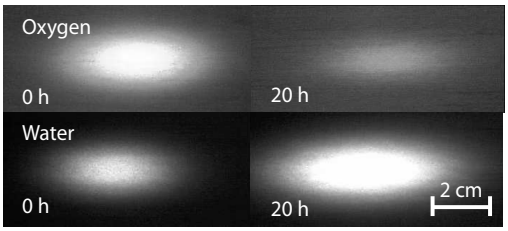

(b)

Fig. 7. (a) Absorption spectrum of 1 cm pure water reproduced from the measurements by Matcher *et al.* [23]. (b) Images of the sample on the detection side for oxygen (760 nm) and water vapor (980 nm) during its drying process.

The 760 nm light is off-resonance from the broad liquid water absorption as shown in Fig. 7(a), and bulk absorption due to the water is small, in strong contrast to the case for 980 nm. The high initial light level can be seen owing to the index-matching effect of the water in the pores, which reduces the lateral scattering and allows more light to reach the detector. As the wood dries the scattering increases and less and less light reaches the detector. Steady-state

#67781 - $15.00 USD Received 3 February 2006; revised 28 March 2006; accepted 3 April 2006
(C) 2006 OSA

conditions then prevail in the dry wood. The significant change in the light levels, as well as the normalized WMS signals for both wavelengths when the wood is nearly dry can be interpreted as the final dry-up of the finest compartments long after the tube structure that contained most of the water has dried up. The scattering increases a lot due to the appearance of small pores of size comparable with the wavelength. This reduces the detected 760 nm light level. Also the 980 nm light level changes due to the continued loss of bulk water absorption.

The dynamics of the transmitted light levels at the two wavelengths could also be studied using near-IR imaging of the transmitted light using standard Web cameras (Q-Tec 100). The transmitted light blobs at 980 nm and 760 nm are shown in Fig. 7(b) for fully wet and fully dry (waiting 20 h = 1200 min) conditions. The intensity in the center of the blobs (where the detector is situated) is related to the intensities given in Fig. 6(c); the 760 nm signal is greatly reduced and the 980 nm is increased. The final levels (20 h) correspond to an attenuation by the sample of the incident light of about 80% for the 980 nm signal and 99.95% for the 760 nm signal. These attenuations suggest that the wood sample thicknesses accessible in transmission measurements cannot be considerably larger than 1 cm for most wood types. For thicker samples the backscattering geometry is still applicable. From recordings, such as the ones shown in Fig. 7(b), information of the spatial distribution can also be extracted and compared with theory [7]. However, a detailed analysis of the spatial distribution is outside the scope of the present paper.

6. Conclusions and discussion

Removing moisture from materials is of major importance in fields as diverse as industrial processing, handling of construction materials, and preparation of agricultural products. The origin of excess water is frequently connected to material porosity. Optical measurement techniques are attractive since they are nonintrusive and frequently deliver data in real time. However, quantitative absorption spectroscopy is hampered by the strong scattering in inhomogeneous materials, making the Beer–Lambert law not directly applicable. In the present paper we have demonstrated the application of the GASMAS technique applied in transmission for the monitoring of water vapor in wood, using corresponding molecular oxygen measurements as a reference. The wavelengths used for the free gas monitoring, 980 nm and 760 nm, are also on- and off-resonant for a broad liquid water absorption feature, and thus information of the bulk water is also obtained. The signal intensities observed can mostly be interpreted as the result of the interplay between specific absorption and scattering, both changing during the drying process. In particular, the time when all the free water has evaporated from the wood can be readily identified by a steep falloff in the water vapor signal accompanied by the reaching of a high-level plateau in the molecular oxygen signal. The ratio between these signals, being dimensionless and largely independent of scattering, shows in particular the arrival at a fully dry sample. This situation is also identified in the differential optical absorption signal for liquid water, with a sharp increase of an order of a magnitude in the ratio of the (broadband) signal intensities at 980 nm and 760 nm.

It is thus clear that optical spectroscopy can be a valuable tool for the practical monitoring of drying processes while also yielding additional information on specifics of drying. For the practical application of the method, measurements in back-scattering geometry (as already applied in our sinusitis monitoring [15]) is of great interest. In order to further elucidate the interplay between scattering and absorption, time-resolved measurements of the photon history in the wood for the two wavelengths would provide independent information on the scattering of the material and the liquid water contents. Such measurements can be performed using white light [6,9], capturing the full spectrum, or employing a number of pulsed diode lasers selected at appropriate wavelengths [24].

#67781 - $15.00 USD Received 3 February 2006; revised 28 March 2006; accepted 3 April 2006
(C) 2006 OSA

Acknowledgement

The authors thank Rita Wallén from the Department of Cell and Organism Biology of Lund University for her help with the microscope pictures. We also acknowledge useful discussions with Lars-Olof Nilsson from the Division of Building Materials of the Lund Institute of Technology.

This work was supported by the Swedish Research Council and the Knut and Alice Wallenberg Foundation.

#67781 - $15.00 USD Received 3 February 2006; revised 28 March 2006; accepted 3 April 2006
(C) 2006 OSA